NASA-TM-107079

NASA Technical Memorandum 107079

Analysis of the Defect Structure of B2 FeAl Alloys

Guillermo Bozzolo
Analex Corporation
Brook Park, Ohio

John Ferrante and Ronald D. Noebe
Lewis Research Center
Cleveland, Ohio

Carlos Amador
Universidad Nacional Autónoma de México
Distrito Federal, México

October 1995

National Aeronautics and
Space Administration

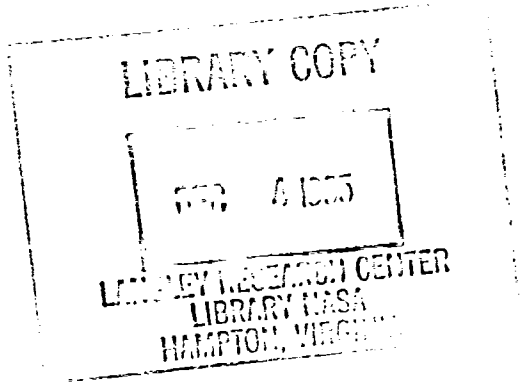

ANALYSIS OF THE DEFECT STRUCTURE OF B2 FeAl ALLOYS

Guillermo Bozzolo[1], John Ferrante[2] and Ronald D. Noebe[2], Carlos Amador[3],
[1]Analex Corporation, 3001 Aerospace Parkway, Brook Park, OH 44142-1003
[2]National Aeronautics and Space Administration, Lewis Research Center, Cleveland, OH 44135.
[3]Facultad de Química, Universidad Nacional Autónoma de México, Ciudad Universitaria, 04510 Distrito Federal, México

Introduction

The defect structure of B2 FeAl has been the subject of several experimental [1-4] and more numerous but conflicting theoretical studies [5-12]. Some support the contention that FeAl is a triple defect forming compound. For Fe-rich alloys, the Al-sublattice is always fully occupied, therefore, when an excess of Fe occurs it will substitute on Al sites with no significant composition dependent vacancy concentration occurring on either sublattice. But with excess Al, vacant sites or constitutional vacancies are formed in the Fe-sublattice. For example, the lattice parameter measurements for FeAl as a function of stoichiometry [1-4] show a peak occurring at the stoichiometric Fe-50 at. % Al composition, with a linearly decreasing lattice parameter on either side of stoichiometry. This behavior is consistent with a triple defect forming compound [5]. Further arguments in favor of a triple defect structure are based on the large heat of formation of FeAl [5,6] and early theoretical work by Neumann et al. [7,8] using a pair-wise interactions model for the study of point defects also favors the formation of triple defects in FeAl.

Other studies support the notion that FeAl is an antistructure or substitutional defect structure compound, where the element in excess locates on the lattice site of the minority element. Work by Kim [9], Weber et al.[10] and Ho and Dodd [4] indicate that structural vacancies in the FeAl system are extremely unlikely and that the presence of thermal vacancies alone can satisfactorily account for the composition and temperature dependence of the vacancy concentration in FeAl alloys. Furthermore, the results of Hosoda [11] and the first-principles calculations by Fu et al. [12,13] indicate that a triple defect structure model does not adequately describe the structure of FeAl and that antisite defects are preferred at the transitional-metal sites for Al-rich alloys. These results, suggesting that FeAl is a substitutional defect forming compound, are more consistent with the observed slip vector in FeAl alloys.

The absence of substitutional antisite defects at the transition metal sites in confirmed triple defect compounds such as NiAl [5,6,12,14,15] indicates that Al atoms prefer to avoid other Al atoms at the nearest neighbor distance. This is consistent with the usual $\langle 100 \rangle$ slip vector in NiAl [14] since a $\frac{1}{2}\langle 111 \rangle$ partial slip vector would result in nearest neighbor contact between the same type of atoms. FeAl on the other hand deforms by a $\langle 111 \rangle$ slip vector [16], at least at room temperature, which is much more consistent with an antisite defect structure.

Consequently, a strong case can be made for either a triple defect structure or an antisite defect structure in FeAl. Yet, almost all of these studies fail to point out that no matter what the defect structure is on the Al-rich side of stoichiometry, it is not stable over a significant compositional range as any cursory look at the FeAl phase diagram [1,6] will indicate. The B2 structure of the FeAl compound exists to less than a two percent Al-rich deviation in

LMTO results					ECT parameters			
Atom	Lattice Parameter (Å)	Cohesive Energy (eV)	Bulk Modulus (GPa)	Vacancy Energy (eV)	p	α ($Å^{-1}$)	λ (Å)	l (Å)
Fe	2.708	6.410	329	2.95	6	3.2329	0.700	0.2490
Al	3.190	3.942	78	1.80	4	1.8756	1.038	0.3695
BFS parameters: $\Delta_{FeAl} = -0.0671$ $Å^{-1}$, $\Delta_{AlFe} = 0.6500$ $Å^{-1}$								

Table 1: LMTO results, ECT parameters for bcc-based Fe and Al and BFS parameters for FeAl

stoichiometry. This would indicate that neither defect structure could be that stable in the Al-rich end of the FeAl system.

Therefore, the objective of this paper is to provide a consistent description of the defect structure of FeAl by modelling the energetics of this system at zero temperature using the BFS method [15,17]. Several basic issues are covered in this study including determination of the B2 phase field, determination of the defect structure on both sides of stoichiometry, and modelling of the lattice parameter as a function of composition. Furthermore, the energetics of the BFS model provide a rational for the limited structural stability of the B2 compound for Al-rich compositions.

The BFS Method

In this work we follow the same procedure used in a previous application of BFS to the analysis of the defect structure of NiAl alloys [15]. For the sake of brevity and in order to allow for a more detailed discussion of the results, we refer the reader to previous papers that provide a thorough description of the method and its application to specific problems [15,17]. In what follows we provide a brief description of the BFS method sufficient to understand the discussion of the results that follows.

The BFS method is based on the idea that the energy of formation of an alloy is the superposition of individual contributions ε_i of non-equivalent atoms in the alloy [17]: $\varepsilon_i = \varepsilon_i^S + g_i(\varepsilon_i^C - \varepsilon_i^{C_0})$. The first term is the *strain* energy ε_i, computed with equivalent crystal theory (ECT) [18], that accounts for the actual geometrical distribution of the atoms surrounding atom i, computed as if all its neighbors were of the same atomic species, and a *chemical* energy $\varepsilon^C - \varepsilon^{C_0}$, which takes into account the fact that some of the neighbors of atom i may be of a different chemical species. For ε_i^C we interpret the chemical composition as a defect of an otherwise pure crystal. We represent this defect by 'perturbing' the electronic density in the overlap region between dissimilar atoms and locating them at equilibrium lattice sites of atom i. To free the chemical energy of structural defect energy, which should only be included in the strain energy, we reference ε_i^C to a similar contribution where no such perturbation is included ($\varepsilon_i^{C_0}$). The coupling function g_i, which ensures the correct asymptotic behavior of the chemical energy, is defined as $g_i = e^{-a_i^S}$, where a_i^S is a solution of $\varepsilon_i^S = -E_C^i \left[1 - (1 + a_i^S)exp(-a_i^S)\right]$ [19], and where E_C^i is the cohesive energy for atom i. In the context of BFS, the terms 'strain' and 'chemical' represent quite different effects than the usually assigned meanings. The BFS strain energy is related to the usual strain only in that the atomic locations are those found in the actual alloy: the BFS strain energy of a given atom is then the actual strain that it would have in a monatomic crystal of the same species of the reference atom. Likewise, the BFS chemical contribution is related to the usual chemical energy in that the actual chemical composition of the alloy is taken into account, but with the neighboring atoms located in ideal atomic sites: the BFS chemical energy of a given atom is then the actual chemical energy in an ordered environment with a lattice spacing characteristic of the equilibrium lattice of the reference atom. The parameters needed by the BFS method, (including the ECT parameters) were calculated using the Linear Muffin-Tin Orbitals (LMTO) method [20] in the Atomic Sphere Approximation (ASA) and are listed in Table 1. For brevity, we refer the reader to Ref. 18 for a detailed discussion on the parameterization of the BFS method.

Results and Discussion

The BFS calculation was performed on a 72 atom cell, allowing for isotropic atomic relaxation induced by the presence of vacancies and substitutional atoms. Instead of searching for an absolute energy minimum for a given composition, we chose to construct a large number of 'candidate', high symmetry, distributions to obtain information on the energetics of the system close to the ground state. This is done with the intention of identifying possible metastable states, in addition to the ones corresponding to ideal thermal equilibrium. For example, if configurations C_1 and C_2 both have negative heats of formation, with $\Delta H_{C_1} < \Delta H_{C_2}$, then configuration C_2 might still appear in the actual alloy with a certain probability, which is lower than that for C_1. If the set of configurations sampled is sufficiently large and the structures are chosen respecting the symmetries that characterize the system, one would expect to find the ground state, or states sufficiently close to it, for each composition. In order to concentrate on the focus of this paper, we leave the details on this computer simulation approach for a forthcoming publication. Examples of the atomic distributions for many of the candidate states are illustrated in Fig. 1, and include combinations of Fe and Al antisite defects as well as Fe and Al vacancies.

Fig. 1 also displays the heat of formation as a function of Al concentration for the set of 'candidate' configurations examined. The results of the simulation are summarized as follows:

1)The BFS results predict the range of composition for the B2 phase field in excellent agreement with experiment. No negative energy states were found beyond 52 at. % Al. There seems to be no limit on the Fe-rich side where the heat of formation first decreases in magnitude and then increases again for higher Fe contents, possibly hinting at the existence of the Fe_3Al ordered ($D0_3$) structure. For those compositions consisting of stoichiometric FeAl or Fe-rich alloys, the lowest energy configurations were those composed of anitsite defect structures.

2) For Al-rich alloys, the antisite defect (Al in Fe sites) was found to have the lowest energy (configuration (b)). A few other configurations with only slighlty smaller values for the heat of formation were found ((c)-(d)). These configurations consisted of arrangements of structural vacancies with only a slightly smaller energy than for the antisite defect structure. All Al-rich structures exhibited much smaller energies than configurations on the Fe-rich side of stoichiometry. The sudden termination of the B2 field at $x_{Al} \sim 52$ at. % can be explained in terms of the BFS contributions to the energy of formation as described in Eq. (1), and shown in Fig. 2. In this figure, the total BFS strain and chemical energies per atom are displayed for the lowest energy states for each composition. The total energy of formation is also shown. The BFS strain contribution shows a very slight monotonic increase with Al content throughout the whole range of the B2 field, due probably to the greater abundance of large Al atoms. In contrast, the BFS chemical energy shows a discontinuous jump for $x_{Al} > 50$ at. %. In this region, substitutional Al atoms occupying Fe sites eliminate chemically favorable (a negative contribution from $e^C - e^{C_0}$ in Eq. (1)) Fe-Al bonds, while at the same time increasing the (always positive) BFS strain due to their larger size. The increasing strain reduces the magnitude of the coupling function g (which links the strain and chemical components) thus emphasizing the loss in negative chemical energy. These combined effects drive the total energy of formation up, quickly saturating the ability to absorb additional Al substitutional atoms. On the Fe-rich side, the opposite is true: substitutional Fe antisite atoms eliminate favorable Fe-Al bonds as well, but the loss in negative chemical energy is offset by the decreasing BFS strain and the subsequent increase in the magnitude of the coupling function.

3) Being a T=0 K calculation the ground state for stoichiometric FeAl naturally corresponds to a perfectly ordered B2 structure. The only other configurations with (much smaller) negative heat of formation corresponds to an antisite defect structure. The triple defect structure (two vacant Al sites plus an Al antisite atom) is even more unlikely, with a nearly positive heat of formation. The small value of the heat of formation for this type of defect, relative to the corresponding one for the ordered B2 structure or even the antisite structure, hints to the unlikelihood of finding this defect in the actual alloy. Consequently, these results are consistent with other theoretical predictions such as Fu et al. [12,13] which conclude that the triple defect structure is energetically unfavorable, but our results also indicate that the triple defect structure is not energetically impossible.

4) For Fe-rich FeAl the substitutional Fe-antisite atom is the main defect type, in agreement with all previous studies. Several configurations of Fe-antisite defects, very close in energy, exist for each composition. The difference between these configurations resides in the relative position of the Fe antisite atoms. As shown in Fig. 3, where diagrams showing the configurations studied for $x_{Al} = 44.44\%$, slight gains in energy are obtained as the additional Fe atoms

accomodate themselves so as to maximize the correlation between them. In other words, the energy slightly lowers as the Fe atoms agglomerate. With even further deviations from stoichiometry the gap between different configurations widens with decreasing Al content indicating the preference for a particular ordering pattern for the Fe-antisite atoms (as the one found for Fe_3Al, which corresponds to the DO_3 ordered structure).

5) A decrease in lattice parameter with Fe content is also found in this calculation, in agreement with the the trend found experimentally. While there is very good agreement for Al-rich alloys, the rate of decrease of the lattice parameter with increasing Fe content is higher than the one observed experimentally. Fig. 4 compares the experimental values of Refs. 1-4 with the ground-state values for the theoretical lattice parameter obtained with BFS. The difference between the measured and computed values of the lattice parameter as a function of composition can be explained in terms of several arguments, including the fact that this calculation was done at T=0 K and that no local relaxation effects (i.e. small displacements of individual atoms around the defect) were included. In addition, consistent with the previous discussion, the clustering of several structures (as shown in Fig. 3) with slightly different order patterns close to the ground state suggest that a fair comparison to experimental results should include the effect of these structures which individually induce an increase in the lattice parameter. Finally, the actual lattice parameter measurements may be influenced by the thermal vacancies that are quenched into FeAl alloys in large numbers [4,11-13] but are not taken into account in our calculations. These factors, when accounted for, could only improve the quality of the agreement between experiment and the present theoretical analysis.

Conclusions

A good understanding of the factors influencing the atomic structure of FeAl or any other ordered system is necessary if further conclusions regarding physical and mechanical properties are to be derived from any given calculation. Our calculation for FeAl seems compatible with most of the evidence gathered through the years, agreeing on the essential facts (correct prediction of the B2 phase field, antisite substitutional defects for all compositions, decrease of the lattice parameter with increasing Fe content) as well as giving some indication on the probability of other defect structures.

References

1. F. Lihl and H. Ebel, Arch. Eisenhuttenw. **32** (1961)483.
2. A. Taylor and R. M. Jones, J. Phys. Chem. Solids **6** (1958) 16.
3. A. J. Bradley and A. H. Jay, J. Iron Steel Inst. **125** (1932) 339.
4. K. M. Ho and R. A. Dodd, Scr. Met. **12** (1978) 995.
5. J. P. Neumann, Acta Metall. **28** (1980) 1165.
6. Y. A. Chang, J. P. Neumann, Prog. Solid State Chem. **14** (1982) 221.
7. P. Neumann, Scripta Metall. **10** (1976) 917.
8. P. Neumann, Y. A. Chang and C. M. Lee, Acta Metall. **24** (1976) 593.
9. S. M. Kim, J. Phys. Chem. Solids **49** (1988) 65.
10. D. Weber, M. Meurtin, D. Paris, A. Fourdeux and P. Lesbats, J. Phys. C: **7** (1977) 332.
11. H. Hosoda, K. Inoue, Y. Mishima, Mat. Res. Soc. Symp. Proc. **364** (1995) 483.
12. C. L. Fu, Y. Y. Ye, M. H. Yoo and K. M. Ho, Phys. Rev. B **48** (1993) 6712.
13. C. L. Fu and J. Zou, Mat. Res. Soc. Symp. Proc. **364** (1995) 91.
14. R. D. Noebe, R. R. Bowman and M. V. Nathal, Inter. Maters. Rev. **38** (1993) 193.
15. G. Bozzolo, C. Amador, J. Ferrante and R. D. Noebe, Scr. Metall. Mater. (in press).
16. Y. Umakoshi and M. Yamaguchi, Philos. Mag. A **41** (1980) 573; *ibid.*, Philos. Mag. A **44** (1981) 711.
17. G. Bozzolo and J. Ferrante, J. Computer-Aided Mater. Design **1** (1993) 305, and references therein.
18. J. R. Smith, T. Perry, A. Banerjea, J. Ferrante and G. Bozzolo, Phys. Rev. B **44** (1991) 6444.
19. J. H. Rose, J. R. Smith and J. Ferrante, Phys. Rev. B **28** (1983) 1835.
20. See, for example, O. K. Andersen, A. V. Postnikov and S. Y. Savrasov, Mat. Res. Soc. Symp. Proc. **253** (1992) 37.

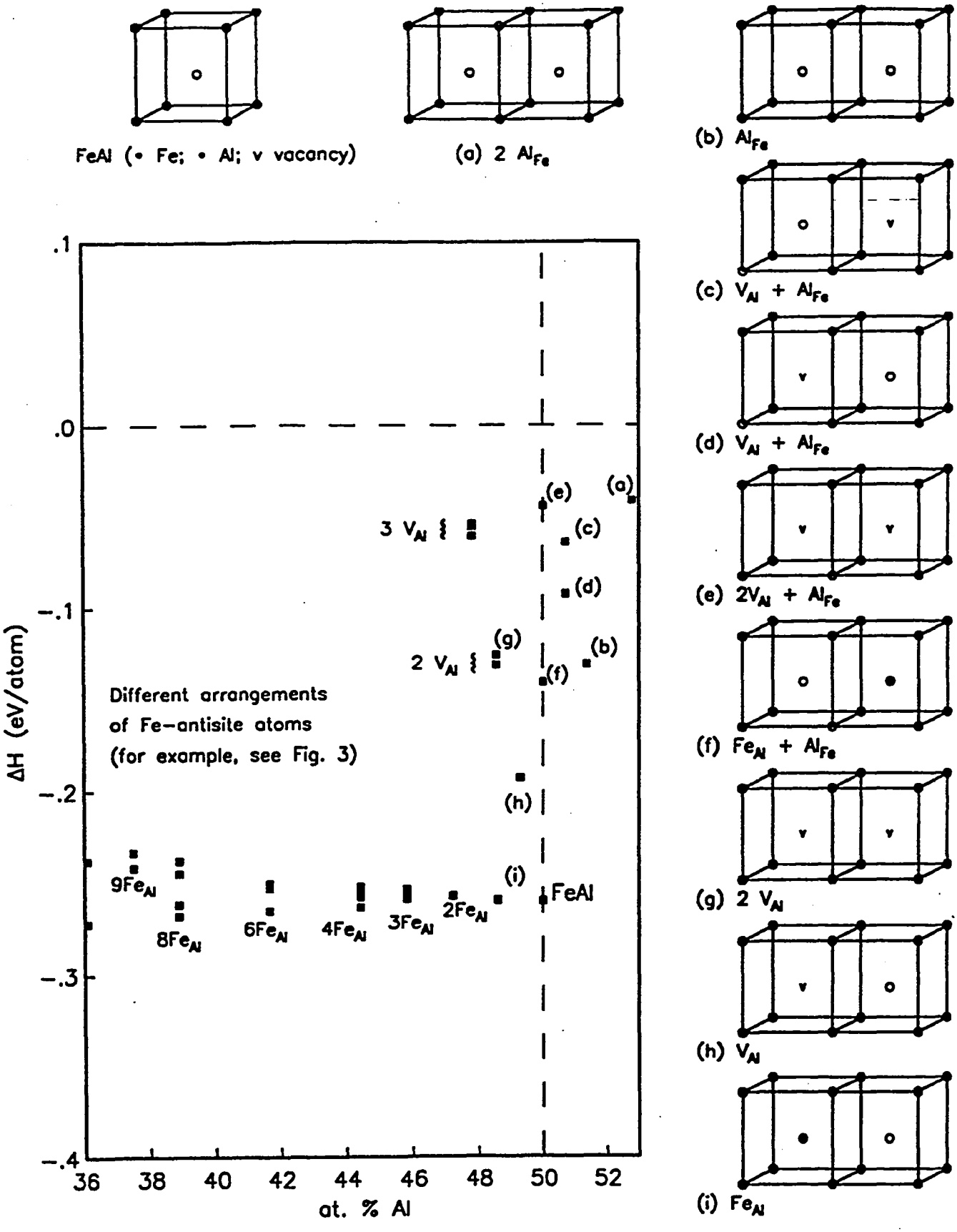

Fig. 1: Heat of formation per atom (in eV/at) as a function of Al concentration for FeAl alloys. The diagrams represent the defect structure of some of the states shown. Fe atoms are indicated with closed circles, Al atoms with open circles.

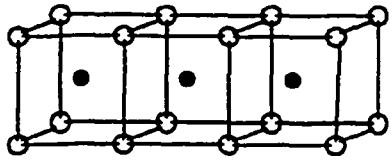

(a) −0.26052 eV/at; 2.908 Å

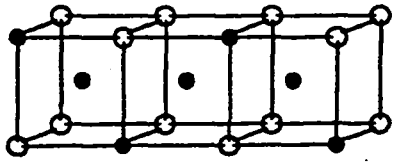

(b) −0.27566 eV/at; 2.874 Å

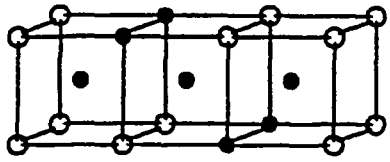

(c) −0.26547 eV/at; 2.874 Å

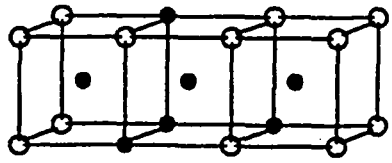

(d) −0.26115 eV/at; 2.874 Å

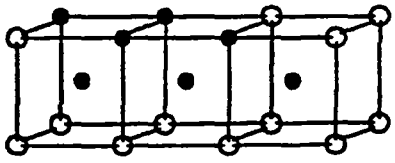

(e) −0.26044 eV/at; 2.875 Å

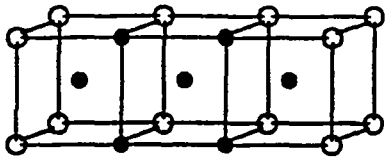

(f) −0.25594 eV/at; 2.876 Å

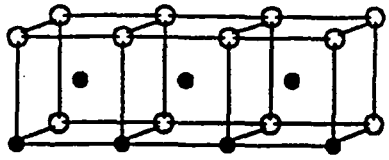

(g) −0.25518 eV/at; 2.876 Å

Fig. 3: (a) Stoichiometric B2 FeAl. (b)–(c): Six configurations with 44.44 at. % Al. The lowest energy configuration is (b), with a heat of formation of −0.27566 eV/atom. The other diagrams ((c)–(g)) differ in the relative position of the four Fe–antisite atoms. Fe atoms are indicated with closed disks and Al atoms with open circles.

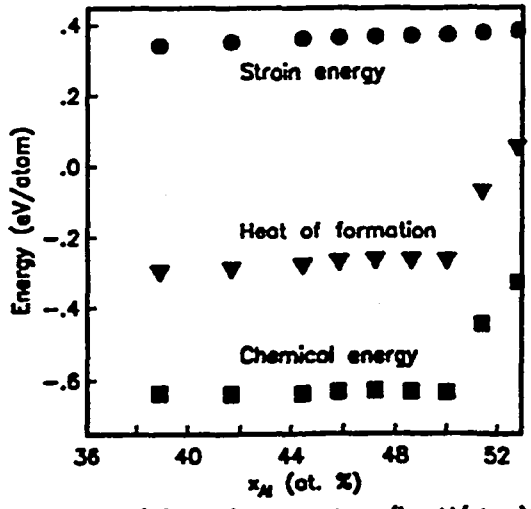

Fig. 2: Heat of formation per atom (in eV/atom) as a function of Al concentration for the ground state structures for each composition. The BFS strain and chemical energies are also shown.

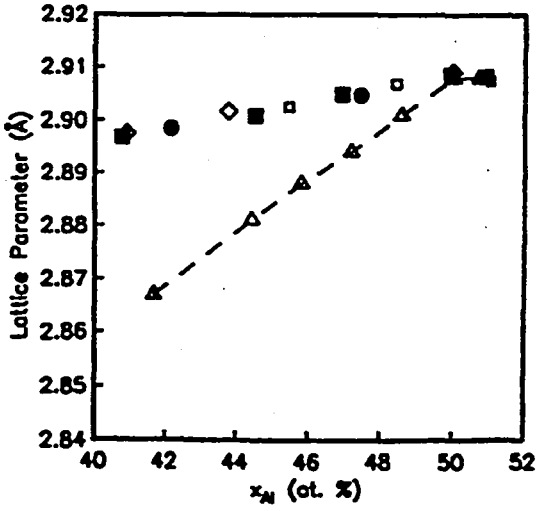

Fig. 4: Experimental (•:[1]; o:[2]; ◦:[3]; □:[4]) and theoretical (Δ) values of the lattice parameter as a function of composition.

REPORT DOCUMENTATION PAGE

Form Approved
OMB No. 0704-0188

1. AGENCY USE ONLY (*Leave blank*)	2. REPORT DATE	3. REPORT TYPE AND DATES COVERED
	October 1995	Technical Memorandum

4. TITLE AND SUBTITLE

Analysis of the Defect Structure of B2 FeAl Alloys

5. FUNDING NUMBERS

WU-505-90-53

6. AUTHOR(S)

Guillermo Bozzolo, John Ferrante, Ronald D. Noebe, and Carlos Amador

7. PERFORMING ORGANIZATION NAME(S) AND ADDRESS(ES)

National Aeronautics and Space Administration
Lewis Research Center
Cleveland, Ohio 44135-3191

8. PERFORMING ORGANIZATION REPORT NUMBER

E-9954

9. SPONSORING/MONITORING AGENCY NAME(S) AND ADDRESS(ES)

National Aeronautics and Space Administration
Washington, D.C. 20546-0001

10. SPONSORING/MONITORING AGENCY REPORT NUMBER

NASA TM-107079

11. SUPPLEMENTARY NOTES

Guillermo Bozzolo, Analex Corporation, 3001 Aerospace Parkway, Brook Park, Ohio 44142 (work funded by NASA Contract NAS3-25776); John Ferrante and Ronald D. Noebe, NASA Lewis Research Center; Carlos Amador, Universidad Nacional Autónoma de México, Facultad de Química, Cuidad Universitaria, 04510 Distrito Federal, México. Responsible person, John Ferrante, organization code 0130, (216) 433-6069.

12a. DISTRIBUTION/AVAILABILITY STATEMENT

Unclassified - Unlimited
Subject Category 26

This publication is available from the NASA Center for Aerospace Information, (301) 621-0390.

12b. DISTRIBUTION CODE

13. ABSTRACT (*Maximum 200 words*)

The BFS method for alloys is applied to the study of the defect structure of B2 FeAl alloys. First-principles Linear Muffin Tin Orbital calculations are used to determine the input parameters to the BFS method used in this work. The calculations successfully determine the phase field of the B2 structure, as well as the dependence with composition of the lattice parameter. Finally, the method is used to perform 'static' simulations where instead of determining the ground state configuration of the alloy with a certain concentration of vacancies, a large number of candidate ordered structures are studied and compared, in order to determine not only the lowest energy configurations but other possible metastable states as well. The results provide a description of the defect structure consistent with available experimental data. The simplicity of the BFS method also allows for a simple explanation of some of the essential features found in the concentration dependence of the heat of formation, lattice parameter and the defect structure.

14. SUBJECT TERMS	15. NUMBER OF PAGES
Alloys; Defects; Semiempirical methods; Iron-aluminum	08
	16. PRICE CODE: A02

17. SECURITY CLASSIFICATION OF REPORT	18. SECURITY CLASSIFICATION OF THIS PAGE	19. SECURITY CLASSIFICATION OF ABSTRACT	20. LIMITATION OF ABSTRACT
Unclassified	Unclassified	Unclassified	